

Lattice thermal expansion studies on single-phase compositions in CeO_2 – ThO_2 – ZrO_2 system

V. Grover, A.K. Tyagi*

Applied Chemistry Division, Bhabha Atomic Research Centre, Mumbai 400085, India

Received 8 May 2004; received in revised form 23 May 2004; accepted 2 July 2004

Available online 7 April 2005

Abstract

Earlier we reported the phase relations in the CeO_2 – ThO_2 – ZrO_2 system under slow cooled conditions from 1400 °C; ceria was used as a surrogate material for plutonia. A number of single-phase compositions with fluorite-type structure were identified in this pseudo-ternary system. For example, about 5 and 20 mol% of zirconia could be dissolved in the lattice of thorium and ceria, respectively. 10 mol% zirconia was incorporated in the lattice of $\text{Th}_{0.5}\text{Ce}_{0.5}\text{O}_2$. The lattice thermal expansion behaviour of a number of single-phase compositions in the temperature range from 293 to 1473 K, as investigated by high temperature XRD, are reported. For example, the average lattice thermal expansion coefficient of pure thorium was found to be 9.58×10^{-6} , which increased to $11.91 \times 10^{-6} \text{ K}^{-1}$ in the composition $\text{Th}_{0.05}\text{Ce}_{0.90}\text{Zr}_{0.05}\text{O}_2$.

© 2005 Elsevier Ltd and Techna Group S.r.l. All rights reserved.

Keywords: B. X-ray methods; C. Thermal expansion; E. Nuclear applications

1. Introduction

The development of uranium-free, inert matrix fuel is of worldwide interest. By using this concept it is possible to annihilate the large stock of plutonium available from dismantled weapons and accumulated stocks from nuclear power plants. Several groups are engaged in development of new inert matrix fuel host lattices [1–5]. Kleykamp [6] has written a review on selection of materials as diluents for “burning” the plutonium. This concept is also being contemplated to prepare targets for transmutation of minor actinides. The inert matrix, as suggested by its name, does not lead to the formation of fissile material after irradiation. To act as an inert matrix has to satisfy a number of stringent conditions, e.g., good neutron economy, have superior thermophysical properties (high thermal conductivity, low thermal expansion, etc.), lack of phase changes and no decomposition at higher temperature, have compatibility with the cladding material, stability against radiation, good

mechanical properties, low leachability and low cost. A number of host lattices are being considered to act as an inert matrix, for diluting plutonium, viz., multi-phase ceramic–ceramic composites (MCC) based on zirconia, alumina or magnesia, $\text{Al}_5\text{Y}_3\text{O}_{12}$, MgO , MgAl_2O_4 , ROX (rock-like oxides) [7]. Several nitrides, carbides [5] and phosphates [8] are also being contemplated to act as an inert matrix.

India has very large deposits of thorium, which is potentially useful for nuclear power production. Being a very stable oxide (chemically inert), thorium could also be considered as a potential host for diluting and burning plutonia, though it is not exactly an inert matrix. The inclusion of thorium is likely to improve the neutron economy and in situ produced U-233 would increase the burnup of the inert matrix-based fuel [9]. Recently, pseudo-ternary phase relations in the CeO_2 – ThO_2 – ZrO_2 system were reported [10] under slow-cooled conditions. Ceria is used as a surrogate material [11] in place of plutonia. The main difficulties while investigating PuO_2 based systems are its high radioactivity and toxicity. One way to overcome this problem is the use of CeO_2 in place of PuO_2 as they both have quite similar physico-chemical properties viz., ionic

* Corresponding author. Tel.: +91 22 2550 5151; fax: +91 22 2559 5330.
E-mail address: akyagi@magnum.barc.ernet.in (A.K. Tyagi).

size in octahedral and cubic coordination, melting points, standard enthalpy of formation and specific heat, etc.

The possibility of presence of Ce^{3+} is quite remote under the experimental conditions employed in the present investigations, i.e., heating at 1400 °C followed by slow cooling in static air. Zhou and Rahman [12] have convincingly concluded based on TG data that CeO_2 does not show an appreciable oxygen loss up to 1400 °C. In fact, these authors have shown that it is nano-crystalline ceria, which shows an appreciable weight loss at about 1300–1400 °C. We have used a micron to sub-micron size ceria in the present investigation, which is known to become slightly sub-stoichiometric ($\text{CeO}_{1.995}$) only at 1500 °C [13]. Based on refinement of the XRD data in $\text{CeO}_2\text{--ThO}_2\text{--ZrO}_2$ [10], several phase regions namely of cubic solid solutions, two-phase and multi-phase regions could be delineated. Ceria and thoria have appreciable solubilities of nominal compositions $\text{Th}_{0.5}\text{Zr}_{0.5}\text{O}_2$ and $\text{Ce}_{0.5}\text{Zr}_{0.5}\text{O}_2$, respectively, whereas the ZrO_2 structure does not accommodate any $\text{Ce}_{0.5}\text{Th}_{0.5}\text{O}_2$. A cubic solid solution phase field and a two-phase field (cubic + monoclinic) could be delineated unequivocally. The single-phase ternary compositions, as found in this study, are expected to be superior to the multiphase compositions for plutonium utilization. Thermal expansion behaviour is an important thermo-physical property, which governs the design and performance of the nuclear fuel pins. In this communication we report on the lattice thermal expansion behaviour of single phase compositions in the $\text{CeO}_2\text{--ThO}_2\text{--ZrO}_2$ system, as studied by high temperature X-Ray diffraction (XRD), in the temperature range from 20 to 1200 °C.

2. Experimental

CeO_2 , ZrO_2 and ThO_2 (all 99.9%) were used as the starting materials. About 10 single phase compositions in $\text{CeO}_2\text{--ThO}_2\text{--ZrO}_2$ system were prepared by a three stage heating protocol. Starting materials were heated at 900 °C for overnight and were well characterized by powder XRD before use. The intimately ground mixtures were heated in the pellet form at 1200 °C for 36 h, followed by second heating at 1300 °C for 36 h after regrinding and repelletising. In order to attain a better homogeneity, the products obtained after second heating were again reground, pelletised and heated at 1400 °C for 48 h, which was the final annealing temperature of all the specimens. The heating and cooling rates were 2 degrees per minute in all the annealing steps and atmosphere was static air. The XRD patterns were recorded on a Philips X-ray diffractometer (Model PW 1710) with monochromatized $\text{Cu K}\alpha$ radiation ($K\alpha_1 = 1.5406 \text{ \AA}$ and $K\alpha_2 = 1.5444 \text{ \AA}$). The silicon was used as an external standard for calibration of the instrument. The XRD patterns were well analyzed by comparing with the reported ones. The lattice parameters were refined by a least squares method.

The high temperature X-ray diffraction (HT-XRD) patterns of the sample were recorded using an X'pert PRO XRD unit fitted with an Anton Parr high temperature attachment. A platinum heater was used as the stage for the sample. A Pt/PtRh(13:87) thermocouple spot welded to the bottom of the stage was used to measure the temperature. The temperature was controlled with an accuracy of $\pm 1 \text{ K}$ using a Eurotherm temperature controller. The XRD patterns ($15^\circ < 2\theta < 80^\circ$, scan time 60 min) were recorded at various temperatures in the range of 20–1200 °C at an interval of 150 °C after holding the sample for 5 min at each desired temperature, in static air. The unit cell parameters at each temperature were determined using a least squares refinement program. The cell volume as well as the coefficients of average lattice thermal expansion were also evaluated.

3. Results and discussion

The lattice parameters of these samples at 20 °C were reported earlier [10]. XRD patterns of each sample, recorded at different temperatures, were refined to determine variations of the lattice parameter as a function of temperature. The lattice parameters for different temperatures were fitted as function of temperature using a second order regression and the fittings are given below (a in nm, T in K).

For $\text{Th}_{0.05}\text{Zr}_{0.05}\text{Ce}_{0.90}\text{O}_2$:

$$a_T = 0.5389 + (5.526 \times 10^{-6})T + (6.103 \times 10^{-10})T^2 \quad (1)$$

For $\text{Th}_{0.10}\text{Zr}_{0.10}\text{Ce}_{0.80}\text{O}_2$:

$$a_T = 0.5406 + (4.911 \times 10^{-6})T + (9.308 \times 10^{-10})T^2 \quad (2)$$

For $\text{Th}_{0.15}\text{Zr}_{0.15}\text{Ce}_{0.70}\text{O}_2$:

$$a_T = 0.5396 + (5.589 \times 10^{-6})T + (4.536 \times 10^{-10})T^2 \quad (3)$$

For $\text{Th}_{0.45}\text{Zr}_{0.10}\text{Ce}_{0.45}\text{O}_2$:

$$a_T = 0.5472 + (5.315 \times 10^{-6})T + (5.785 \times 10^{-10})T^2 \quad (4)$$

For $\text{Th}_{0.75}\text{Zr}_{0.125}\text{Ce}_{0.125}\text{O}_2$:

$$a_T = 0.5557 + (4.108 \times 10^{-6})T + (7.359 \times 10^{-10})T^2 \quad (5)$$

For $\text{Th}_{0.80}\text{Zr}_{0.10}\text{Ce}_{0.10}\text{O}_2$:

$$a_T = 0.5561 + (3.885 \times 10^{-6})T + (1.087 \times 10^{-9})T^2 \quad (6)$$

For $\text{Th}_{0.95}\text{Zr}_{0.05}\text{O}_2$:

$$a_T = 0.5580 + (3.709 \times 10^{-6})T + (8.630 \times 10^{-10})T^2 \quad (7)$$

For $\text{Zr}_{0.10}\text{Ce}_{0.90}\text{O}_2$:

$$a_T = 0.5367 + (4.879 \times 10^{-6})T + (1.409 \times 10^{-9})T^2 \quad (8)$$

For $\text{Zr}_{0.20}\text{Ce}_{0.80}\text{O}_2$:

$$a_T = 0.5342 + (4.971 \times 10^{-6})T + (1.356 \times 10^{-9})T^2 \quad (9)$$

It may be noted that the lattice parameters of these compounds at 20 °C calculated using these equation is within the standard deviation compared to those reported in a previous work [10].

The average lattice thermal expansion coefficients, α_a (20–1200 °C), are given in the Table 1; α_a values decrease progressively on increasing the ThO_2 content in this series, which can be attributed to the lower α_a values of thorium. It may be noted that thorium is a high melting point solid and, in general, the coefficient of average thermal expansion is inversely proportional to the melting point of the solid [15]. A typical plot of lattice thermal expansion (%) as a function of temperature for $\text{Th}_{0.15}\text{Zr}_{0.15}\text{Ce}_{0.70}\text{O}_2$ is shown in Fig. 1. The observed lattice thermal expansion (%) for each sample was fitted as a function of temperature using a polynomial regression and the fittings are given as follows (T in K).

For $\text{Th}_{0.05}\text{Zr}_{0.05}\text{Ce}_{0.90}\text{O}_2$:

$$100 \times \Delta a/a = -0.19503 + (5.17454 \times 10^{-4})T + (4.78399 \times 10^{-7})T^2 + (1.80663 \times 10^{-10})T^3 - (1.66445 \times 10^{-13})T^4 \quad (10)$$

Table 1

Average lattice thermal expansion coefficients (293–1473 K) for different compositions

Composition	$\alpha_a (\times 10^6)$	Reference
$\text{Th}_{0.05}\text{Ce}_{0.90}\text{Zr}_{0.05}\text{O}_2$	11.91	Present work
$\text{Th}_{0.10}\text{Ce}_{0.80}\text{Zr}_{0.10}\text{O}_2$	11.72	Present work
$\text{Th}_{0.15}\text{Ce}_{0.70}\text{Zr}_{0.15}\text{O}_2$	11.58	Present work
$\text{Th}_{0.45}\text{Ce}_{0.45}\text{Zr}_{0.10}\text{O}_2$	11.19	Present work
$\text{Th}_{0.75}\text{Ce}_{0.125}\text{Zr}_{0.125}\text{O}_2$	9.75	Present work
$\text{Th}_{0.80}\text{Ce}_{0.10}\text{Zr}_{0.10}\text{O}_2$	9.88	Present work
$\text{Th}_{0.95}\text{Zr}_{0.05}\text{O}_2$	9.24	Present work
$\text{Ce}_{0.9}\text{Zr}_{0.1}\text{O}_2$	13.7	Present work
$\text{Ce}_{0.8}\text{Zr}_{0.2}\text{O}_2$	13.9	Present work
ThO_2	9.58	[14]
CeO_2	12.68	[14]
ZrO_2	8.0 ^a	[16]

^a Average linear thermal expansion coefficient (298–1353 K).

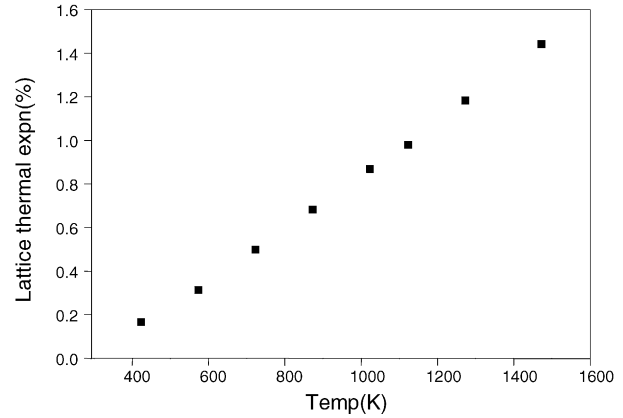


Fig. 1. Lattice thermal expansion behaviour of $\text{Th}_{0.15}\text{Ce}_{0.70}\text{Zr}_{0.15}\text{O}_2$ as a function of temperature.

For $\text{Th}_{0.10}\text{Zr}_{0.10}\text{Ce}_{0.80}\text{O}_2$:

$$100 \times \Delta a/a = -0.18551 + (2.38911 \times 10^{-4})T + (1.69058 \times 10^{-6})T^2 + (-1.29339 \times 10^{-9})T^3 + (3.80623 \times 10^{-13})T^4 \quad (11)$$

For $\text{Th}_{0.15}\text{Zr}_{0.15}\text{Ce}_{0.70}\text{O}_2$:

$$100 \times \Delta a/a = -0.35758 + (0.00133)T + (-4.25685 \times 10^{-7})T^2 + (3.95626 \times 10^{-10})T^3 + (-1.05474 \times 10^{-13})T^4 \quad (12)$$

For $\text{Th}_{0.45}\text{Zr}_{0.10}\text{Ce}_{0.45}\text{O}_2$:

$$100 \times \Delta a/a = -0.22478 + (7.47123 \times 10^{-4})T + (-7.62746 \times 10^{-8})T^2 + (6.06365 \times 10^{-10})T^3 + (-2.81623 \times 10^{-13})T^4 \quad (13)$$

For $\text{Th}_{0.75}\text{Zr}_{0.125}\text{Ce}_{0.125}\text{O}_2$:

$$100 \times \Delta a/a = -0.21088 + (5.57639 \times 10^{-4})T + (6.61271 \times 10^{-7})T^2 + (-5.50729 \times 10^{-10})T^3 + (1.84242 \times 10^{-13})T^4 \quad (14)$$

For $\text{Th}_{0.80}\text{Zr}_{0.10}\text{Ce}_{0.10}\text{O}_2$:

$$100 \times \Delta a/a = -0.11661 + (3.79676 \times 10^{-5})T + (1.455 \times 10^{-6})T^2 + (-9.2383 \times 10^{-10})T^3 + (2.2987 \times 10^{-13})T^4 \quad (15)$$

For $\text{Th}_{0.95}\text{Zr}_{0.05}\text{O}_2$:

$$100 \times \Delta a/a = -0.68902 + 0.00359T \\ + (-5.7085 \times 10^{-6})T^2 \\ + (4.72072 \times 10^{-9})T^3 \\ + (-1.31849 \times 10^{-12})T^4 \quad (16)$$

For $\text{Zr}_{0.10}\text{Ce}_{0.90}\text{O}_2$:

$$100 \times \Delta a/a = -0.31599 + (0.00107)T \\ + (7.43119 \times 10^{-9})T^2 \\ + (1.56701 \times 10^{-10})T^3 \\ + (-3.19838 \times 10^{-14})T^4 \quad (17)$$

For $\text{Zr}_{0.20}\text{Ce}_{0.80}\text{O}_2$:

$$100 \times \Delta a/a = -0.27786 + (7.28723 \times 10^{-4})T \\ + (9.53573 \times 10^{-7})T^2 \\ + (-7.86106 \times 10^{-10})T^3 \\ + (2.73782 \times 10^{-13})T^4 \quad (18)$$

However, the average lattice thermal expansion coefficient of ceria increases on substituting 10 and 20 mol% zirconia. This observation is somewhat different than what one expects based on the thermal expansion coefficients of the end members.

4. Conclusions

Nine single phasic compositions were investigated for lattice thermal expansion behaviour by high temperature-

XRD. These compositions represent the thorium and ceria rich regions in the single-phase fields. The lattice thermal expansion data generated in this study can be used to simulate the thermal expansion behaviour of the corresponding plutonia-based compositions.

References

- [1] H. Akie, T. Muromura, H. Takano, S. Matsura, *Nucl. Technol.* 107 (1994) 182.
- [2] J.M. Paratte, R. Chawla, *Ann. Nucl. Energy* 22 (1995) 471.
- [3] C. Lombardi, A. Mazzola, *Ann. Nucl. Energy* 23 (1996) 1117.
- [4] K. Ferguson, *Trans. Am. Nucl. Soc.* 75 (1996) 75.
- [5] M. Burghartz, H. Matzke, C. Leger, G. Vambenepe, M. Rome, *J. Alloys Compd.* 544 (1998) 271.
- [6] H. Kleykamp, *J. Nucl. Mater.* 275 (1999) 1.
- [7] C. Degueudre, J.M. Paratte, *J. Nucl. Mater.* 274 (1999) 1.
- [8] K. Bakker, H.J. Hein, R.J.M. Konings, R.R. van der Laan, H. Matzke, P. Van Vlaanderen, *J. Nucl. Mater.* 252 (1998) 228.
- [9] F. Vettriano, G. Magnani, T. La Torretta, E. Marmo, S. Coelli, L. Luzzi, P. Ossi, G. Zappa, *J. Nucl. Mater.* 274 (1999) 23.
- [10] V. Grover, A.K. Tyagi, *J. Nucl. Mater.* 305 (2002) 83.
- [11] Y.W. Lee, H.S. Kim, S.H. Kim, C.Y. Young, S.H. Na, G. Ledergerber, P. Heimgarbner, M. Pouchon, M. Burghartz, *J. Nucl. Mater.* 274 (1999) 7.
- [12] Zhou, Rahman, *Acta Mater.* 45 (1997) 3635; Zhou, Rahman, *J. Mater. Res.* 8 (1993) 1680.
- [13] H.J. Matzke, V.V. Rondinella, T. Wiss, *J. Nucl. Mater.* 274 (1999) 47.
- [14] A.K. Tyagi, B.R. Ambekar, M.D. Mathews, *J. Alloys Compd.* 337 (2002) 275.
- [15] L.G.V. Uitert, H.M. O'Bryan, M.E. Lines, H.J. Guggenheim, G. Zydig, *Mater. Res. Bull.* 12 (1977) 261.
- [16] J.W. Shackelford, W. Alexander (Eds.), *CRC Mater. Sci. Eng. Hand Book*, third ed., CRS Press, Washington.